Current Biology 19, 1660–1664, October 13, 2009 ©2009 Elsevier Ltd All rights reserved DOI 10.1016/j.cub.2009.07.070

Report

Local Interactions Lead to Pathogen-Driven Change to Host Population Dynamics

Michael Boots,[1,*] Dylan Childs,[1] Daniel C. Reuman,[2] and Michael Mealor[1]
[1]Animal and Plant Sciences, University of Sheffield, Western Bank, Sheffield S10 2TN, UK
[2]Ecology and Evolution Section, Imperial College London, Silwood Park, Ascot SL5 7PY, UK

Summary

Individuals tend to interact more strongly with nearby individuals or within particular social groups. Recent theoretical advances have demonstrated that these within-population relationships can have fundamental implications for ecological and evolutionary dynamics [1–11]. In particular, contact networks are crucial to the spread [12–14] and evolution [8, 9, 11, 15] of disease. However, the theory remains largely untested experimentally [16]. Here, we manipulate habitat viscosity and thereby the frequency of local interactions in an insect-pathogen model system in which the virus had previously been shown to have little effect on host population dynamics [16, 17]. At high viscosity, the pathogen caused the collapse of dominant and otherwise stable host generation cycles. Modeling shows that this collapse can be explained by an increase in the frequency of intracohort interactions relative to intercohort interactions, leading to more disease transmission. Our work emphasizes that spatial structure can subtly mediate intraspecific competition and the effects of natural enemies. A decrease in dispersal in a population may actually (sometimes rather counterintuitively) intensify the effects of parasites. Broadly, because anthropological and environmental change often cause changes in population mixing, our work highlights the potential for dramatic changes in the effects of parasites on host populations.

Results and Discussion

We investigated how spatial structure impacts on a host-parasite interaction through the manipulation of host population viscosity. By using an established laboratory host-parasite model system [18, 19] consisting of the Indian meal moth *Plodia interpunctella* and its granulosis virus larval parasite (PiGV), we varied the degree of local interactions within experimental populations. In microcosms, larvae live and move within a food medium while adults emerge and fly above the food; adults mix completely and cannot be infected. Typically generational host population cycles occur [18, 20] driven by asymmetric competition including cannibalism among larval stages [21], although the cycles are less apparent under poor resource conditions [22]. The virus is transmitted among larvae through consumption of free-living virus and through necrophagy of infected individuals. In all previous experiments (none of which manipulated food viscosity), the virus had only minor effects on host dynamics [18, 23].

*Correspondence: m.boots@sheffield.ac.uk

We manipulated larval population spatial structure both with and without the virus [16]. Starting from standard medium used in previous experiments (here called soft food), we developed two more viscous media (here called intermediate and hard food: see Experimental Procedures). The effect of food viscosity on the movement rate of early instar larvae was measured in experimental lanes. Increased viscosity significantly reduced larval movement rate (Figure 1), which would lead to more local interactions within the microcosms. *Plodia* eggs are laid in batches, so increasingly localized interactions were expected to lead in turn to an increase in within-cohort interactions relative to between cohort interactions. We found no effect of food viscosity on larval development time, pupal weight, or survivorship: our manipulation altered spatial structure without affecting individual fitness (Figure 1).

Microcosms of the host were established with one of the three food viscosities either in the presence (five replicates for each food medium) or absence (three replicates for each medium) of PiGV. Dead adult host population sizes were recorded once a week for 40 weeks. In the absence of virus, all host populations showed the same pattern of strong generational cycles (Figures 2 and 3). Cycling in soft-, intermediate-, and hard-food replicates had similar and not significantly different mean dominant periods, respectively: 38.02 (SD 1.24), 36.98 (SD 1.40), and 41.82 (SD 2.95) days (ANOVA, $p = 0.057$; Welch test $p = 0.180$). Mean adult population sizes were, respectively, 147.72 (SD 10.62), 126.90 (SD 10.83), and 98.07 (SD 1.91); differences were significant (Welch test, $p = 0.011$). The soft-food values were similar to previous experiments on soft food carried out over longer time periods [18, 23], demonstrating the robustness of the system. Overall, manipulation of food viscosity in the absence of PiGV altered population size and may have slightly altered the dominant cycle period, but did not qualitatively change dynamics (Figures 2 and 3).

For microcosms that included the virus, generational cycles were again dominant in soft- and intermediate-viscosity food (Figures 2 and 3). In line with previous results [18, 23], there was no significant change in the dominant period of the infected populations relative to the disease-free populations when both fed on soft food (38.02 to 39.31 days; SD 1.24 to 0.90). Considering only soft- and intermediate-food treatments with and without virus, two-way ANOVA revealed that interaction effects and virus main effects on dominant period were not significant ($p = 0.291$, 0.343, respectively): the virus did not affect cycling for these food types. However, host dynamics in the presence of virus in hard food were very different: generational cycles were substantially modified and obscured in all but one of the replicate populations (Figures 2 and 3). A two-way ANOVA on the log power of the generational cycle frequency revealed significant interaction effects ($p = 0.013$) resulting from the loss of the cycles in the hard-food treatments with the virus. In addition there is evidence of longer-period oscillations in all virus-present, hard-food replicates (Figures 2 and 3), not present for other experimental treatments or in previous experiments. In summary, the virus had a qualitatively substantial effect on population

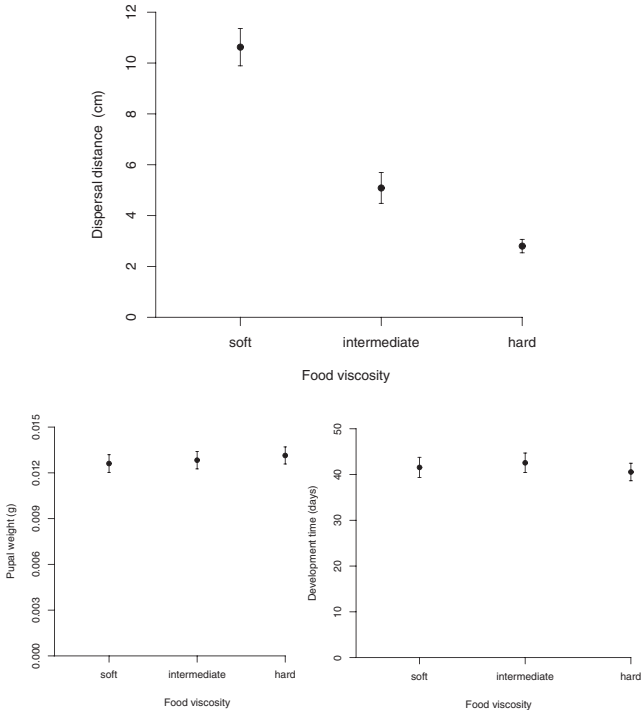

Figure 1. The Effect of the Spatial Manipulation

The effect of food viscosity on mean distance moved (top), mean pupal weight (bottom left), and mean development time (bottom right). Error bars are standard errors. Increasing viscosity caused significant change in larval dispersal distance (ANOVA on log transformed data; $F_{2,82} = 52.86$, $p < 0.001$). Food viscosity did not affect pupal weight (ANOVA; $F_{2,121} = 0.22$, $p = 0.80$), survivorship (generalized linear model with binomial errors; $F_{2,3} = 6.92$, $p = 0.13$), or larval development time ($F_{2,177} = 0.23$, $p = 0.79$).

dynamics, but only when host movement rates were sufficiently reduced.

The increased viscosity has therefore caused the parasite to have a much stronger impact on the host population dynamics. We know that altering the viscosity of the food media has not affected the host growth rate of individuals (Figure 1) and is therefore unlikely to have significantly affected host demography. The change in dynamics is therefore due either to changes in parasite characteristics or to a change in the spatial interactions between host and parasite. The virus evolved lower infectivity in the most viscose populations (35). It would be a counterintuitive explanation, however, that lower transmission of the parasite leads to a more dramatic impact of the virus on host dynamics. It is likely that the change in the mixing of the population has caused the increased effect of the parasite on host population dynamics. In particular, increased viscosity of the population is likely to lead to an increase in interactions between individuals of the same stage/age. Adults lay eggs in batches within the microcosm, and as a consequence, in the more viscose food media, individuals will be less able to move away from individuals of the same cohort. A well developed stage-structured model [21] explains generational cycles in *Plodia interpunctella* as resulting from asymmetric competition between young and older larvae (with cannibalism its most extreme form) and larvae-on-egg cannibalism [21]. We now develop this modeling approach to test whether an increase in relative intracohort interactions is enough to explain our results. Because we do not have good data on the actual spatial relationships within the microcosms, we do not build an explicitly spatial model of the delay differential stage-structured system. Rather, we model the effect of space implicitly by altering the relative intra- to intercohort interaction rates within the existing well-defined and parameterized modeling framework.

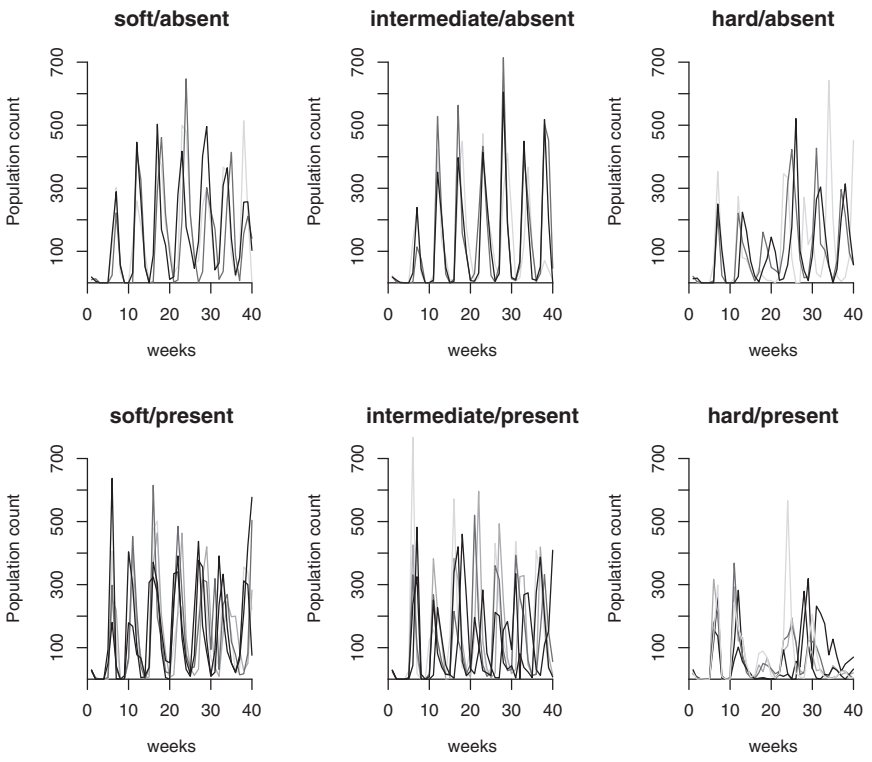

Figure 2. Population Time Series

Weekly dead adult population counts of *Plodia interpunctella* in each microcosm under different food-viscosity and virus treatments. Replicates are plotted in shades of gray. Generational cycles dominate dynamics except for hard-food, virus-present replicates, where generational cycles are suppressed or intermittent.

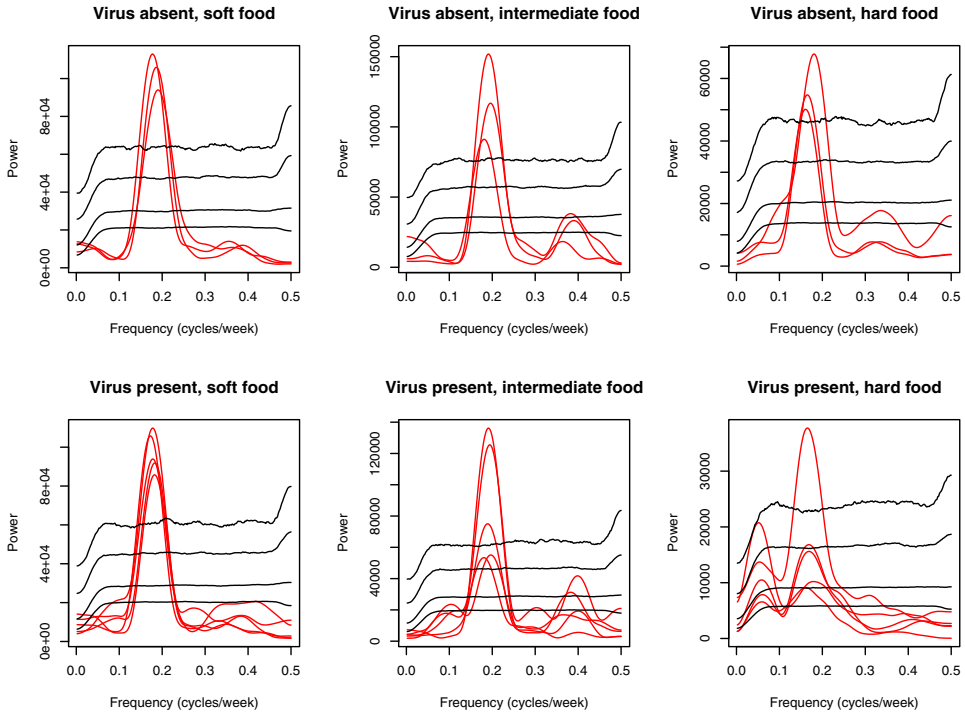

Figure 3. Spectral Analysis of Time Series Data

Red lines are the power spectra of the experimental time series, and black lines are 50th, 75th, 95th, and 99th percentiles of power spectra for the null hypothesis that data came from white noise with the same stationary distribution as data for each treatment. All replicates showed significant or marginally significant generation cycles except four hard-food, virus-present replicates. Peaks at frequency 0–0.1 cycles/week in the hard-food, virus-present replicates are evidence of long-period oscillations (see text), which correspond to apparent long-period modulation of generational cycles, visible especially at around week 20 in the hard-food, virus-present replicates. Qualitatively similar modulation also occurred in model simulations (Figure 4, text).

Analysis of the single-species *Plodia interpunctella* model shows that the possible dynamics are generational cycles, half generational cycles, or no cycles, with the observed generational cycles predicted in our soft-food regimen (43). It is easy to show that increasing the strength of competition within cohorts relative to between cohorts decreases average population size. This process may therefore parsimoniously explain the average population reductions seen in our virus-free, hard-food microcosms relative to our virus-free soft-food microcosms (Figures 3 and 4). We next developed a host-pathogen model of our system (Supplemental Data available online) by building on the host-only model [21]. It is well established that early larval instars are more susceptible to infection and produce fewer virus occlusion bodies than older instars because of their smaller size [24]. We model transmission within the susceptible larval class, with different contact rates at the different viscosities. We find that increasing the overall strength of competition in the host-parasite model again reduced average population sizes but did not lead to the collapse of generational cycles, except at unrealistically high competition levels. This suggests that competition alone is unlikely to have caused our results and that the interaction with the parasite has been important. When we increase the within-stage interactions within our host-parasite model (Supplemental Data), we find the collapse of generational cycles (Figure 4). When higher viscosity leads to more interactions within a stage, which in turn leads to higher infection rates, the breakdown of the cohort structure and therefore the loss of the generational cycles (Figure 4) is seen.

We have shown that a change in mixing in our populations leads to a dramatic parasite-driven change in population dynamics. There is considerable interest in how processes at the individual scale affect population dynamics. Here we show that variation in spatial structure leads to group level effects on population-scale processes mediated through competition, stage structure, and infection. Adults moved freely in all treatments of this study and therefore we have demonstrated that spatial structure is important not only in extreme spatial scenarios; subtle changes can also have important effects. Anthropomorphic and environmental change, habitat fragmentation, and increasing global travel are altering mixing patterns within human and animal populations. Understanding the impact of changes in mixing on the transmission of parasites and pathogens is particularly important given the continued threat of infectious disease. The world is likely to continue to get "smaller" and more connected. Our results demonstrate that these changes can lead to radically different and unexpected population dynamics through interactions with natural enemies: a parasite that had no effect on host population dynamics at one level of mixing altered dynamics entirely at another level of mixing.

More generally, our results emphasize the importance of interactions between the environment and disease and the central importance that spatial structure may play in ecology and epidemiology. A decrease in dispersal in a population through, for instance, habitat fragmentation, leading to an increase in the relative frequency of local interactions may intensify the effects of parasites. This is surprising because

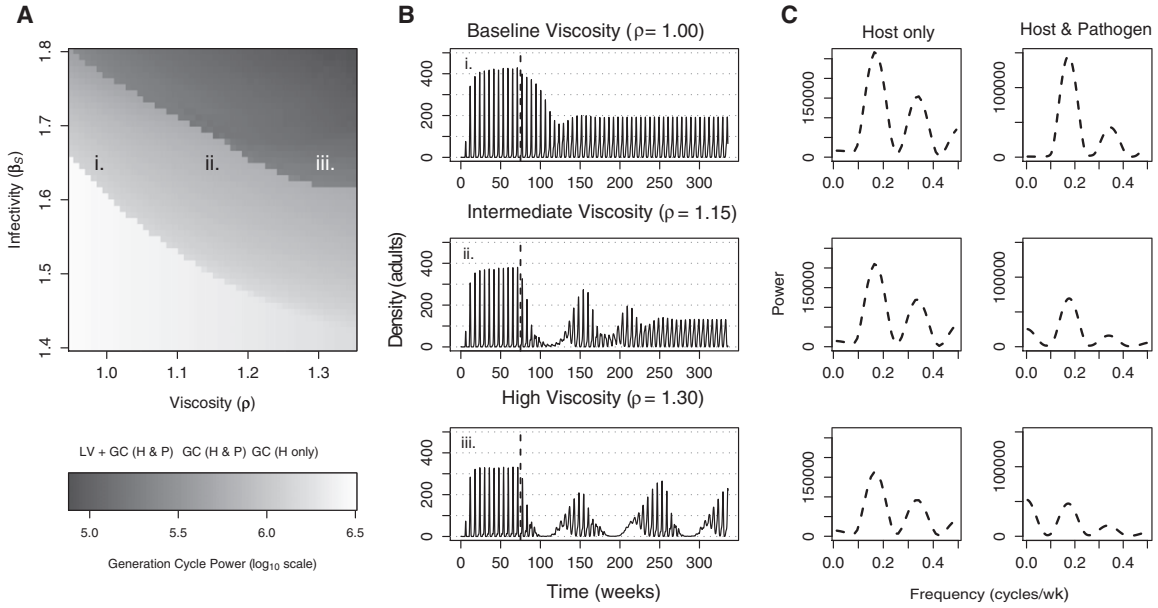

Figure 4. The Results from the Model

(A) Stability diagram as a function of food viscosity, ρ, and parasite infectivity, β_S. The diagram delineates the separate dynamic regimes (GC, generation cycles; LV + GC, mixture of Lotka-Volterra and generation cycles), highlights the region of disease persistence (H & P, disease present; H only, disease free), and shows the amplitude of the generation-cycle component of dynamics.

(B) Example model dynamics exhibiting the transition from pure generation cycles to more complex dynamics with increasing viscosity: top, generation cycle (GC) dynamics generated by the canonical parameter set (see Supplemental Data); middle, reduced amplitude generation cycle (GC) dynamics; bottom, mixture of long-period Lotka-Volterra cycles and generation cycles. Densities are total numbers of living adults. A single infected larva was introduced after 75 weeks (vertical dashed line), such that host dynamics in the absence of virus are exhibited in the region left of the vertical dashed lines.

(C) Power spectra of plotted model output in (B) for the adult host dynamics in the absence (left) or presence (right) of the virus. Note the increased power at low frequencies for the hard-food, virus-present simulation, paralleling a qualitatively similar pattern of increased low-frequency power in Figure 3.

increased disease impact is generally associated with greater population dispersal. Our work also emphasizes the lack but importance of manipulative spatial experiments in ecology and evolution. Broadly, since anthropological and environmental changes often cause changes in population mixing, our work highlights the potential for dramatic changes in the effects of parasites on host populations.

Experimental Procedures

Manipulation of Viscosity

Food medium of three viscosities were produced by adding water to the standard rearing media. The standard larval medium is a 400 g HiPP organic harvest breakfast cereal, 80 g brewers yeast, 100 ml glycerol, 100 ml organic clear honey, 0.5 g sorbic acid (an antibacterial agent), and 0.5 g methyl paraben (a fungicide). Adding 60 ml of distilled water produced the intermediate-viscosity medium used in the experiments; adding 140 ml of distilled water produced the high-viscosity medium. A series of arenas with four lanes were established, each 18 cm long and 4 cm wide and filled with one of the media to a depth of 0.5 cm. Movement rates were measured by placing one first-instar larvae at one end of each lane. Lanes were covered; movement on top of the food or between lanes was not possible. Each 4-lane box was placed in an aerated plastic container in an incubator at 27°C ± 2°C and 35% ± 5% humidity for 12 days. The media in each lane was destructively sampled 1 cm at a time along its entire 18 cm length and the distance moved was recorded. In total there were 30 replicate boxes used, and 40 *Plodia* larvae were tested at each of the three food viscosities. Individual development time and pupal weight on the different media was recorded in incubators set at 27°C ± 2°C and 35% ± 5% humidity under abundant food levels to eliminate competition effects.

Microcosms

Twenty-four populations were then established on 170 g of food in 20 × 20 cm plastic containers, with five virus-infected and three virus-free replicates. The medium in each replicate was divided into six sections; one section of food was replaced every week. Replicates were initiated with 15 fifth-instar males and 15 fifth-instar females. For the virus-infected treatments, 12 late-instar, virus-infected cadavers were also placed on the food (two cadavers on each of the six sections). Populations were placed in incubators at 27°C ± 2°C and 35% ± 5% humidity for 40 weeks. Dead adults removed weekly and counted.

Modeling

Our model is based on the well-developed *Plodia interpunctella* stage-structured models of Briggs et al. (2000) [21]. The original model, which explains host dynamics without virus, invoked asymmetric competition among larval cohorts as the primary mechanism maintaining generation cycles. Our new model includes additional variables and equations to model virus transmission within and among larval cohorts. See the Supplemental Data for a complete description of the model. We assume that only the smaller larval class can become infected, adding five extra parameters to the single host model of Briggs et al. (2000) with an additional equation governing the dynamics of the small-infected larvae class, $I_S(t)$:

$$dI_S(t)/dt = R_{I_S}(t) - D_{I_S}(t),$$

where

$$R_{I_S}(t) = \mu_{SS}\beta_S I_S(t) L_S(t)$$

and

$$D_{I_S}(t) = \mu_{SS} I_S(t) L_S(t) + \mu_{LS} I_S(t) L_L(t) + \delta I_S(t).$$

The terms L_s and L_L are the densities of small and large larvae, respectively. Parameters μ_{SS} and μ_{LS} are the per capita per individual consumption rate of I_S by L_S and L_L, β_S is a scalar infectivity parameter describing the linear relationship between the per capita consumption rate and the rate of disease transmission, and δ is the virus activity decay rate. One additional term was also added to account for loss of individuals from the small larvae class through infection.

Supplemental Data

Supplemental Data include Supplemental Experimental Procedures, two figures, and one table and can be found with this article online at http://www.cell.com/current-biology/supplemental/S0960-9822(09)01587-5.

Acknowledgments

We thank Ben Jaques for the R interface to Simon Wood's "Solver" code and the Natural Environmental Research Council for funding.

Received: June 3, 2009
Revised: July 16, 2009
Accepted: July 22, 2009
Published online: October 1, 2009

References

1. Durrett, R., and Levin, S.A. (1994). Stochastic spatial models—a users guide to ecological applications. Philos. Trans. R. Soc. Lond. B Biol. Sci. *343*, 329–350.
2. Tilman D. and Kareiva P., eds. (1997). Spatial Ecology: The Role of Space in Population Dynamics and Interspecific Interactions (Princeton, NJ: Princeton University Press).
3. Sato, K., Matsuda, H., and Sasaki, A. (1994). Pathogen invasion and host extinction in lattice structured populations. J. Math. Biol. *32*, 251–268.
4. Dieckmann U., Law R., and Metz J.A.J., eds. (2000). The Geometry of Ecological Interactions: Simplifying Spatial Complexity (Cambridge: Cambridge University Press).
5. Law, R., Murrell, D.J., and Dieckmann, U. (2003). Population growth in space and time: Spatial logistic equations. Ecology *84*, 252–262.
6. Bolker, B.M., and Pacala, S.W. (1999). Spatial moment equations for plant competition: Understanding spatial strategies and the advantages of short dispersal. Am. Nat. *153*, 575–602.
7. Murrell, D.J., Travis, J.M.J., and Dytham, C. (2002). The evolution of dispersal distance in spatially-structured populations. Oikos *97*, 229–236.
8. Boots, M., Hudson, P.J., and Sasaki, A. (2004). Large shifts in pathogen virulence relate to host population structure. Science *303*, 842–844.
9. Boots, M., and Sasaki, A. (1999). 'Small worlds' and the evolution of virulence: Infection occurs locally and at a distance. Proc. R. Soc. Lond. B. Biol. Sci. *266*, 1933–1938.
10. Haraguchi, Y., and Sasaki, A. (2000). The evolution of parasite virulence and transmission rate in a spatially structured population. J. Theor. Biol. *203*, 85–96.
11. Rand, D.A., Keeling, M., and Wilson, H.B. (1995). Invasion, stability and evolution to criticality in spatially extended, artificial host-pathogen ecologies. Proc. R. Soc. Lond. B. Biol. Sci. *259*, 55–63.
12. Meyers, L.A., Pourbohloul, B., Newman, M.E.J., Skowronski, D.M., and Brunham, R.C. (2005). Network theory and SARS: Predicting outbreak diversity. J. Theor. Biol. *232*, 71–81.
13. Ferguson, N.M., Keeling, M.J., Edmunds, W.J., Gant, R., Grenfell, B.T., Amderson, R.M., and Leach, S. (2003). Planning for smallpox outbreaks. Nature *425*, 681–685.
14. Eames, K.T.D., and Keeling, M.J. (2002). Modeling dynamic and network heterogeneities in the spread of sexually transmitted diseases. Proc. Natl. Acad. Sci. USA *99*, 13330–13335.
15. Read, J.M., and Keeling, M.J. (2003). Disease evolution on networks: The role of contact structure. Proc. R. Soc. Lond. B. Biol. Sci. *270*, 699–708.
16. Boots, M., and Mealor, M. (2007). Local interactions select for lower pathogen infectivity. Science *315*, 1284–1286.
17. Bjornstad, O.N., Sait, S.M., Stenseth, N.C., Thompson, D.J., and Begon, M. (2001). The impact of specialized enemies on the dimensionality of host dynamics. Nature *409*, 1001–1006.
18. Sait, S.M., Begon, M., and Thompson, D.J. (1994). Long-term population dynamics of the Indian meal moth *Plodia interpunctella* and its granulosis virus. J. Anim. Ecol. *63*, 861–870.
19. Begon, M., Sait, S.M., and Thompson, D.J. (1996). Predator-prey cycles with period shifts between two- and three- species systems. Nature *381*, 311–315.
20. Gurney, W.S.C., Nisbet, R.M., and Lawton, J.H. (1983). The systematic formulation of tractable single-species population models incorporating age structure. J. Anim. Ecol. *52*, 479–495.
21. Briggs, C.J., Sait, S.M., Begon, M., Thompson, D.J., and Godfray, H.C.J. (2000). What causes generation cycles in populations of stored-product moths? J. Anim. Ecol. *69*, 352–366.
22. McVean, R.I.K., Sait, S.M., Thompson, D.J., and Begon, M. (2002). Effects of resource quality on the population dynamics of the Indian meal moth *Plodia interpunctella* and its granulovirus. Oecologia *131*, 71–78.
23. Bjornstad, O.N., Begon, M., Stenseth, N.C., Falck, W., Sait, S.M., and Thompson, D.J. (1998). Population dynamics of the Indian meal moth: Demographic stochasticity and delayed regulatory mechanisms. J. Anim. Ecol. *67*, 110–126.
24. Sait, S.M., Begon, M., and Thompson, D.J. (1994). The influence of larval age on the response of *Plodia interpunctella* to a granulosis virus. J. Invertebr. Pathol. *63*, 107–110.

Current Biology, Volume *19*

Supplemental Data

Local Interactions Lead to Pathogen-Driven Change to Host Population Dynamics

Michael Boots, Dylan Childs, Daniel C. Reuman, and Michael Mealor

Supplemental Experimental Procedures

Model Outline

Our baseline host model is derived from the framework developed by Briggs et al (2000). This has successfully described the population dynamics of the *Plodia interpunctella* system and provides a mechanistic explanation for these patterns. Using a lumped age-class approach (Nisbet & Gurney, 1983), the host population is structured into five physiologically distinct life-stages: eggs, 'small' larvae, 'large' larvae, pupae and adults. Larval survival and egg predation are assumed to be density dependent. There are no sources of density-independent mortality in the model as these are thought to be negligible under laboratory conditions. In our implementation, we remove the egg predation term from small larvae, since this makes no significant difference to the dynamics. Briggs et al (2000) demonstrated that asymmetric larval competition and egg predation by large larvae are necessary and sufficient conditions to produce generation cycles of the type observed in laboratory populations of *Plodia interpunctella*, under realistic assumptions about the vital rates.

In order to model the virus dynamics, we include a single infected compartment for the small larval stage, as shown in the schematic (see main text). We make this assumption as the first three *Plodia interpunctella* larval stages (here lumped into 'small larvae') are much more susceptible to infection than the fourth instar, while the fifth instar is unlikely to ever become infected (Sait *et al.* 1994). Although the granulosis virus can persist in the environment, infection within the population cages is often seen to occur when healthy individuals consume infected cadavers (Sait *et al.* 1994). Infected individuals are effectively packages of virus that are transmitted through necrophagy by

healthy ones. We therefore model the infection process via direct consumption of infected cadavers. For simplicity we also assume the absence of a latent period following infection and a linear pathogen transmission function. Briggs and Godfray (1995) have shown that in general that length of latent periods and strength of density dependence in transmission terms will influence the population dynamical outcome in stage-structured host parasite interactions. Increasing the latent period is generally destabilising, while increasing density dependence in the per-capita pathogen efficiency is generally stabilising. Since we do not have access to data summarising these two processes, we adopt the simplest set of assumptions: (1) that the length of the latent period is negligible and (2) that per capita pathogen transmission is density independent such that transmission increases linearly with pathogen density.

Model Formulation

The structure of the model is defined by a set of balance equations describing the rate of change of individuals in the egg stage, $E(t)$, small larval stage, $L_S(t)$, large larval stage, $L_L(t)$, the adult stage $A(t)$, and infected larval stage:

$$\begin{aligned} dE(t)/dt &= R_E(t) - M_E(t) - D_E(t) \\ dL_S(t)/dt &= R_{L_S}(t) - M_{L_S}(t) - D_{L_S}(t) \\ dL_L(t)/dt &= R_{L_L}(t) - M_{L_L}(t) - D_{L_L}(t). \\ dA(t)/dt &= R_A(t) - M_A(t) - D_A(t) \\ dI_S(t)/dt &= R_{I_S}(t) - D_{I_S}(t) \end{aligned} \qquad \text{Eq S1}$$

The equation for each life stage contains three terms: $R_X(t)$, describing the rate of recruitment of individuals into stage X, $M_X(t)$, describing the rate of maturation of individuals out of stage X, and $D_X(t)$ represent the mortality rate in stage X. The mortality term in this framework also includes the rate of infectious larvae, which may occur directly through consumption or via loss of virus activity.

The current adult density multiplied by the female per capita fecundity per day, *r*, gives the recruitment rate of eggs:

$$R_E(t) = rA(t). \qquad \text{Eq S2}$$

The death rate during the egg stage is:

$$D_E(t) = c_{EL} L_L(t) E(t) \quad \text{Eq S3}$$

where c_{EL} is the (linear) per capita rate of egg cannibalism by L_L. The maturation rate out of the egg stage is simply the rate of recruitment into the egg stage τ_E days ago, multiplied by the probability of surviving through the egg stage:

$$M_E(t) = R_E(t - \tau_E) S_E(t) \quad \text{Eq S4}$$

where $S_E(t)$ is the probability of surviving density-dependent egg mortality:

$$S_E(t) = \exp\left\{-\int_{t-\tau_E}^{t} c_{EL} L_L(x) dx\right\}. \quad \text{Eq S5}$$

This can be expressed in differential equation form; such that $S_E(t)$ becomes an additional state variable that is solved simultaneously with the stage-density variables.

The recruitment rate into the small larval stage is equal to the rate of maturation out of the egg stage:

$$R_{L_S}(t) = M_E(t) \quad \text{Eq S6}$$

and the mortality rate during the small larval stage is:

$$D_{L_S} = [c_{SS} L_S + c_{SL} L_L + \mu_{SS} \beta_S I_S] L_S \quad \text{Eq S7}$$

where c_{SS} and c_{SL} are the per capita effects on L_S resulting from competition by L_S and L_L, μ_{SS} is the per capita per individual consumption rate of I_S by L_S, and β_S is a scalar parameter describing the linear relationship between the per capita consumption rate and the rate of disease transmission. The maturation rate out of the small larval class is:

$$M_{L_S}(t) = R_{L_S}(t - \tau_{L_S}) S_{L_S}(t) \quad \text{Eq S8}$$

where $S_{L_S}(t)$ is the probability of surviving density-dependent egg mortality:

$$S_{L_S}(t) = \exp\left\{-\int_{t-\tau_S}^{t} (c_{SS} L_S(x) + c_{SL} L_L(x) + \mu_{SS} \beta_S I_S(x)) L_S(x) dx\right\} \quad \text{Eq S9}$$

An analogous set of equations (without infection terms) describing the recruitment rate, R_{L_L}, mortality rate, D_{L_L}, and maturation rate, M_{L_L}, of large larvae can also be derived in a similar manner; the details of which are omitted here for the sake of brevity.

Since we assume that the adult and pupal mortality rates are negligible, the recruitment rate into the adult class is simply the maturation rate of individuals out of the large larval stage τ_P days ago:

$$R_{L_S}(t) = M_{L_L}(t - \tau_P)$$ Eq S10

and the mortality rate during the adult stage is:

$$D_A(t) = 0\,.$$ Eq S11

The adult stage has a maximum duration of τ_A days, after which all adults are assumed to senesce and die, such that:

$$M_A(t) = R_A(t - \tau_A).$$ Eq S12

Infection of small larvae occurs via consumption of small-infected larval units:

$$R_{I_S} = \mu_{SS}\beta_S I_S(t) L_S(t)$$ Eq S13

This formulation counts infected densities in units of small-infected larvae. Loss of small-infected larvae occurs as a result of virus activity decay and consumption of infectious units by small and large larvae:

$$D_{I_S}(t) = \mu_{SS} I_S L_S + \mu_{LS} I_S L_L + \delta I_S$$ Eq S14

where δ is the virus activity decay rate and μ_{LS} is the per capita per individual consumption rate of I_S by L_L.

Derived parameters

We now explain the derivation of several 'higher-order' parameters, the purpose of which is to simplify presentation and analysis of the model. We have assumed the Lotka-Volterra form of competition, in which the coefficient c_{ij} describes the mortality effect experienced by a stage i individual as a result of each individual in stage j. Each of the four larval competition coefficients in the original Briggs et al (2000) model influences the mean host abundance, but the four terms do not have independent effects on the type of dynamics generated. Briggs et al (2000) demonstrate that for a given set of life history parameters and rate of egg cannibalism, the dynamics of their single species *Plodia* model are uniquely determined by the ratios $\chi = c_{iL}/c_{iS}$ and $\psi = c_{Sj}/c_{Lj}$, where χ describes the asymmetry in the larval competitive effects and ψ describes the asymmetry in the sensitivity to competition.

We follow a similar approach to Briggs et al (2000) and introduce an analogous (but not identical) pair of parameters χ and ψ, along with a third parameter ρ. All three parameters influence the competition coefficients, with the new χ and ψ equal to the original Briggs et al (2000) definition when $\rho = 1$. We introduce ρ to illustrate the hypothesised effect of altering food viscosity; as ρ increases (enhanced viscosity), we wish to trace a path through parameter space in such a way that individuals interact more with those from their own cohort and less with those of alternative cohorts. With this in mind we can define the competition coefficients introduced above in terms of the derived parameters, such that $c_{SS} = c\,\rho$, $c_{SL} = c\,\chi/\rho$, $c_{LS} = c/(\psi\,\rho)$, and $c_{LL} = c\,\chi/(\psi\,\rho)$. The parameter c determines the overall strength of larval competition. It is clear that in the absence of infection, the value of this parameter has no effect on the dynamics of the system, as we can simply rescale the model by a factor c. A similar expression can be derived for the large larva - egg competition term, such that $c_{EL} = c\,\omega/\rho$. Here, the dimensionless parameter ω scales the strength of competition experienced by the egg stage in terms of overall larval competition. We also introduce one further dimensionless parameter, ε, to establishes the per capita per individual consumption rate of infected individuals in terms of the competition parameters, such that, $\mu_{SS} = c_{SS}\varepsilon = c\,\varepsilon\,\rho$ and $\mu_{LS} = c_{SL}\varepsilon = c\,\varepsilon\,\chi/\rho$. Thus, we can see that increasing ρ increases the strength of intra-cohort interactions (c_{SS} and c_{LL}), while concomitantly reducing the strength of inter-cohort interactions (c_{SL}, c_{LS} and c_{EL}). Increasing ρ simultaneously raises the consumption rate of infected larvae by small larvae and reduces consumption by the immune large larvae class, raising the potential for infection.

Finally, we introduce a parameter, Δ, that expresses the average period larvae remain infectious in the absence of consumption, in terms of the generation time of *Plodia*,such that:

$$\delta = \Delta^{-1}\left(\tau_E + \tau_S + \tau_L + \tau_P\right)^{-1}. \qquad \text{Eq S15}$$

This is a more convenient scale on which to examine the effects of the infectious period. Canonical parameters for the model are given in table 1.

Model Dynamics

The dynamics of the model were explored by numerical simulation rather than traditional stability analysis. This reflects the aims of the study, which is concerned primarily with factors influencing both the strength and persistence of a robust dynamic regime (i.e. generation cycles). Each simulation was run for a total of 6500 days. The population was inoculated with 10 uninfected small larvae at time 0, and then a further 10 infected small larvae we're introduced on day 500. The first 2500 days were discarded from subsequent analysis in order to reduce the influence of transients on the system dynamics. In order to reveal the strength of any extant generation cycles we estimated the spectral density of simulated host density time series sampled at daily intervals. For each series, periodograms were calculated using a fast Fourier transform and these were smoothed using a pair of moving average windows of 3 and 5 days. It is important to realise that estimates of the generation cycle amplitude can be used to summarise the extant dynamics at different parameter values when the competition parameter, c, is constant across different simulations. Therefore, for a given value of c, a figure showing the amplitude of the generation cycles as a function of any parameter of interest provides qualitative information about the dynamics (e.g. generation cycles vs generation cycles modulated by Lotka-Volterra, see below). Since the competition parameter does not influence the dynamics *per se*, only mean abundance, we fixed it at the value adopted by Briggs et al (2000) in all simulations. This is a level of competition that leads to population sizes in the models that are similar to those seen in the experimental microcosms. More importantly, we are not currently interested in regions of parameter space that promote stable dynamics or half-generation cycles in the single species case, as these are never observed in the laboratory microcosm. To this end, we fixed the remaining parameters describing host competition (χ, ψ and ω) at values that place the parasite free dynamics firmly inside the region of parameter space at which generation cycles occur (Table 1). The results presented here and in the main text are robust to the exact values chosen for these three competition parameters, assuming we remain in the region promoting generation cycles in the single species case. The remaining *Plodia* specific parameters are identical to those used in the Briggs et al (2000) models.

We now extend the analysis presented in the main text to explore the sensitivity of the model predictions to changes in four key parameters: food viscosity, parasite infectivity, infectious period and the relative consumption rate. We focus on the epidemiological parameters because we know relatively little about these, compared to host life history. Results are presented in Figure S1. Each panel summarises the host population dynamics as a function of parasite infectivity, β_S, and food viscosity, ρ; for a given infectious period, Δ, and consumption rate scaling factor, ε. The central panel (labelled e) is identical to the corresponding figure in the main text. As parasite infectivity and food viscosity increase, travelling from the lower left to the upper right regions within any given panel, we may observe one of four distinct dynamic regimes. At the lower left of each panel there is a light grey region corresponding to disease-free (large amplitude) generation cycles. Clearly, lower parasite infectivity reduces transmission of the parasite and may preclude parasite persistence. Low food viscosity has a similar indirect effect, as this results in low consumption of I_S by L_S, thereby reducing parasite transmission. As we increase β_S and ρ, the next region (medium grey) observed corresponds to reduced amplitude host generation cycles in accompanied by parasite persistence. In this region we may observe decaying Lotka-Volterra cycles, however, host regulatory processes come to dominate the interaction, leading eventually to persistent generation cycles, albeit at reduced-amplitude compared to the disease free case. The third region present in most panels (dark grey region, all panels except panel g) corresponds to mixture of Lotka-Volterra and generational cycles. This appears as parasite mediated regulation of the host starts to become more dominant, as β_S or ρ is further increased. Increasing food viscosity results in greater parasite transmission, while simultaneously reducing inter-cohort (L_S vs. L_L) and increasing intra-cohort competition (L_L vs. L_L and L_S vs. L_S). This second effect alone may result in eventual loss of generation cycles in the parasite free case, but only at much higher viscosity compared to the case where the parasite is present. Finally, sufficient increase in the strength of the host parasite interaction can result in complete loss of the generation cycles (black regions; panels a, c & d). The resultant dynamics may be stable equilibria or Lotka-Volterra cycles; the numerical analysis presented makes no distinction between the two.

The impact of increasing the infectious period, Δ, or the consumption rate of infected larvae, ε, can be seen by moving vertically up or horizontally across panels (left to right), respectively. In common with previous a study of stage-structured host-parasite dynamics (Briggs and Godfrey, 1995), we find that increasing the infectious period reduces the likelihood of generation cycles. Instead, Lotka-Volterra cycles become more likely over comparable regions of parameter space. Increasing the consumption rate of infected larvae also increases the likelihood of Lotka-Volterra cycles, with a concomitant reduction in the likelihood of observing generation cycles in the presence of the parasite. In either case, the impact of altering the food viscosity is essentially unaltered; a clear threshold viscosity exists, associated with a sudden reduction in the amplitude of generation cycles as persistent Lotka-Volterra cycles are initiated.

Table S1. Canonical parameters with their description. Remaining low level parameters are derived from these.

Parameter	Interpretation and source	Value
τ_E	Duration of egg stage *	4.3 days
τ_{L_S}	Duration of small larval stage *	10 days
τ_{L_L}	Duration of large larval stage *	15 days
τ_P	Duration of pupal stage *	7 days
τ_A	Duration of adult stage *	5.5 days
r	Daily adult fecundity *	21 $days^{-1}$
c	Overall strength of competition ^	7.5×10^{-5} L^{-1}
χ	Asymmetry in the larval competitive effects at standard viscosity ^	5
ψ	Asymmetry in the sensitivity to competition at standard viscosity ^	5
ω	Scaling of egg cannibalism relative to overall larval competition ^	40
ε	Scaling of infected consumption relative to larval competition	1.0
β_S	Infectivity of pathogen	1.65
Δ	Uptake-free average infectious period	2.0 generations
ρ	Relative food media viscosity	1.0

* Life history parameters are identical to the canonical set used by Briggs et al (2000, see table 1), which in turn are derived from empirical studies of individual larvae.

^ Canonical competition parameters were chosen to ensure that they lie in a region of parameter space characterised by generation cycles in the absence of the parasite. These cycles are robust, in the sense that small perturbations to the competition parameters cannot destroy generation cycles.

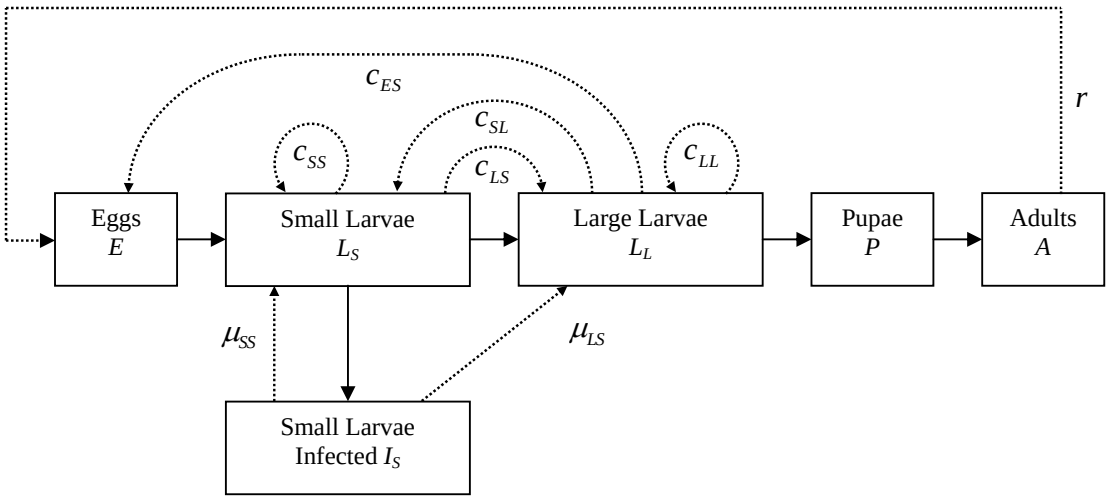

Figure S1. Schematic diagram of the stage structured host-virus model. The labelled boxes represent compartments in the model (*Plodia* life-stages or disease states) with letters corresponding to the appropriate state variable. Interactions among compartments are labelled with dotted arrows, where c_X represents a competition coefficient, μ_X is a consumption rate, and r is adult fecundity.

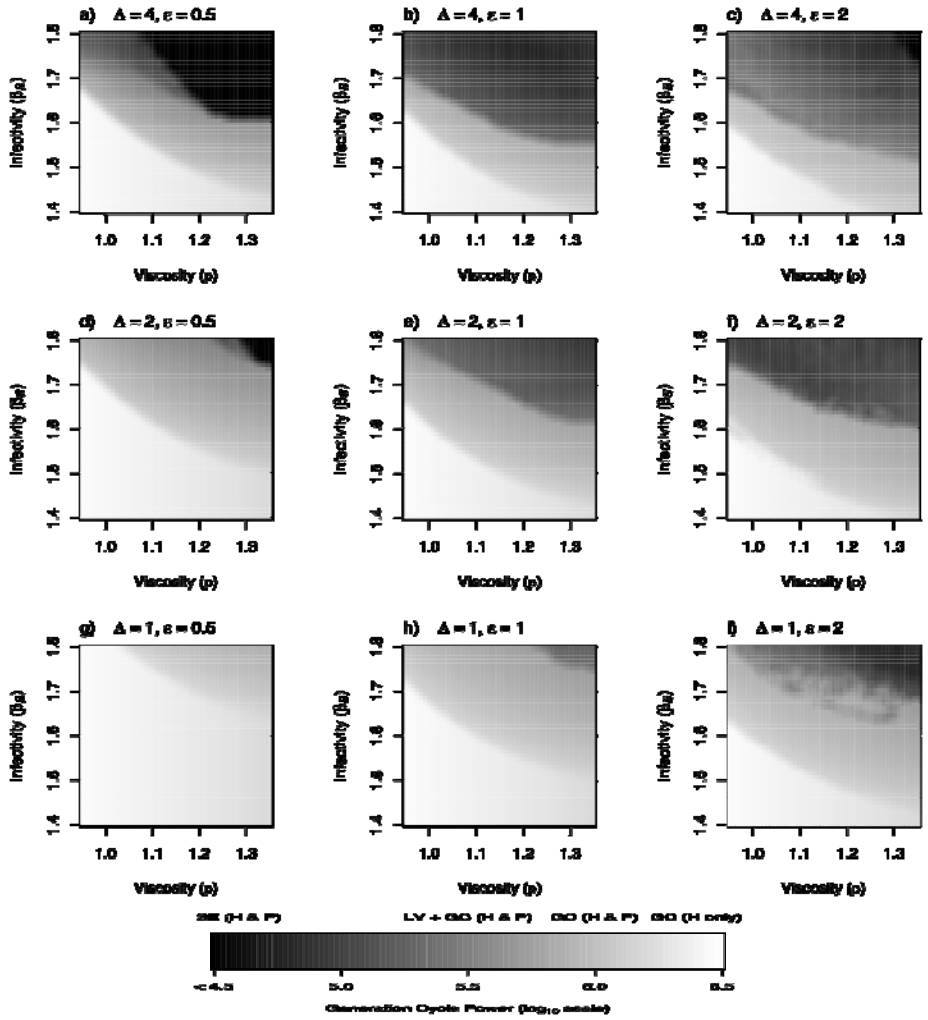

Figure S2. Stability diagrams under the restricted model allowing only small larval infection. These are given as a function of food viscosity, ρ, parasite infectivity in small larvae, β_S, the infectious period, Δ, and the scaling factor for consumption rate, ε. The central panel (labelled e) is identical to the corresponding figure in the main text. The diagram delineates the separate dynamic regimes (GC, generation cycles; LV + GC, mixture of Lotka-Volterra and generation cycles; SE stable equilibria), highlights the region of disease persistence (H & P, disease present; H only, disease free), and shows the amplitude of the generation cycle component of the dynamics. Remaining parameters are as in ***Table S1***.